Toxicology Letters 222 (2013) 197–203

Contents lists available at ScienceDirect

Toxicology Letters

journal homepage: www.elsevier.com/locate/toxlet

No overt structural or functional changes associated with PEG-coated gold nanoparticles accumulation with acute exposure in the mouse heart

Chengzhi Yang[a], Hui Yang[b], Jimin Wu[a], Zenghui Meng[a], Rui Xing[a], Aiju Tian[a], Xin Tian[b], Lijun Guo[a], Youyi Zhang[a], Guangjun Nie[b,**], Zijian Li[a,*]

[a] Institute of Vascular Medicine, Peking University Third Hospital, Key Laboratory of Cardiovascular Molecular Biology and Regulatory Peptides, Ministry of Health, Key Laboratory of Molecular Cardiovascular Sciences, Ministry of Education and Beijing Key Laboratory of Cardiovasicular Receptors Research, Beijing 100191, China

[b] CAS Key Laboratory for Biomedical Effects of Nanomaterials and Nanosafety, National Center for Nanoscience and Technology of China, Beijing 100190, China

HIGHLIGHTS

- Investigated the effects of PEG-coated AuNP on cardiac function, structure and inflammation.
- PEG-coated AuNP had no obvious cardiac toxic effects in normal mice.
- Cardiac AuNPs content increased by 6-fold in the mouse model of cardiac remodeling.
- PEG-coated AuNP had no obvious cardiac toxic effects on the remodeling process.

ARTICLE INFO

Article history:
Received 23 May 2013
Received in revised form 16 July 2013
Accepted 19 July 2013
Available online 29 July 2013

Keywords:
Gold nanoparticles
Heart
Cardiac toxicity
Cardiac remodeling

ABSTRACT

In this study, we investigated the cardiac biodistribution of polyethylene glycol (PEG)-coated AuNPs and their effects on cardiac function, structure and inflammation in both normal and cardiac remodeling mice. The model of cardiac remodeling was induced by subcutaneously injection of isoproterenol (ISO), a non-selective beta-adrenergic agonist, for 7 days. After AuNPs were injected intravenously in mice for 7 consecutive days, Au content in different organs was determined quantitatively by inductively coupled plasma mass spectrometry (ICP-MS), cardiac function and structure were measured by echocardiography, cardiac fibrosis was examined with picrosirius red staining, the morphology of cardiomyocytes was observed with hematoxylin and eosin (H & E) staining. The accumulation of AuNPs in hearts did not affect cardiac function or induce cardiac hypertrophy, cardiac fibrosis and cardiac inflammation under normal physiological condition. Cardiac AuNPs content was 6-fold higher in the cardiac remodeling mouse than normal mice. However, the increased accumulation of AuNPs in the heart did not aggravate ISO-induced cardiac hypertrophy, cardiac fibrosis or cardiac inflammation. These observations suggest that PEG-coated AuNPs possess excellent biocompatibility under both physiological and pathological conditions. Thus, AuNPs may be safe for cardiac patients and hold great promise for further development for various biomedical applications.

1. Introduction

With the speedy development of nanotechnology, the applications of nanomaterials in biomedicine become more critical and are widely employed. Nanoparticles have tremendous potential in biomedical applications, from delivering drugs to novel diagnostic tools for a wide range of diseases (Oberdorster et al., 2005; Prabhu and Patravale, 2012). In particular, gold nanoparticles (AuNPs) have unique chemical and physical properties, such as easy for preparation and functionalization, the excellent stability and biocompatibility and the distinctive optical properties due to surface plasmon oscillation of free electrons (Duncan et al., 2010; Huang et al., 2007). These feasible characteristics endue AuNPs great potential for many biomedical applications, such as drug delivery, biological imaging, biosensing, gene transfection and diagnosis of diseases (Dreaden et al., 2012; Liu and Ye, 2013). Moreover, AuNPs have been explored by the USA National Institute of

* Corresponding author. Tel.: +86 10 82265519.
** Corresponding author. Tel.: +86 10 82545529.
E-mail addresses: niegj@nanoctr.cn (G. Nie), lizijian@bjmu.edu.cn (Z. Li).

0378-4274/$ – see front matter © 2013 Elsevier Ireland Ltd. All rights reserved.
http://dx.doi.org/10.1016/j.toxlet.2013.07.018

Standards and Technology as potential "gold standard" materials for evaluating biological responses to nanosized particles (Khlebtsov and Dykman, 2011). Given that AuNPs hold great promise in biomedicine, the assessment of the biodistribution and potential risks of AuNPs is particularly important.

It is well known that 99% of mouse genes have direct counterparts in humans (Gunter and Dhand, 2002). Genetically modified mouse models can be used in the research of the molecular mechanism of toxicity (Patten and Hall-Porter, 2009; Rusyn et al., 2010). Therefore, mouse model is suitable in the studies of AuNPs toxicology. Several studies have assessed the biodistribution and toxicity of AuNPs in mice. The spherical-shaped AuNPs were detected in various organs including blood, liver, spleen, kidney, testis, thymus, heart, lung and brain (De Jong et al., 2008). Repeated intraperitoneal injection of AuNPs didn't induce subacute damage to the brain, liver, kidney, lungs and spleen in an *in vivo* research (Lasagna-Reeves et al., 2010). AuNPs injected into pregnant mice by tail vein were taken up by the placenta and the fetus (early development stage), but did not cause developmental toxicity (Yang et al., 2012). However, PEG-coated AuNPs were shown to induce acute inflammation and apoptosis in liver (Cho et al., 2009). Therefore, AuNPs-induced toxicity *in vivo* may be different in different organs.

Cardiac diseases are the leading cause of death worldwide. Therefore, many patients with treatment of AuNPs may have accompanied cardiac diseases. However, there have been only a limited number of studies on cardiac toxicity of AuNPs. Especially, there is currently no study on the pathological cardiac toxicity of AuNPs. Therefore, it is critical to assess AuNPs toxicity on both physiological and pathological hearts. Pathological cardiac remodeling, including hypertrophy and fibrosis, is a common pathological feature of many cardiac diseases and an independent risk factor for cardiac morbidity and mortality (Frey and Olson, 2003; van Berlo et al., 2013). Chronic catecholamine stimulation plays a critical role in cardiac remodeling (Jeong et al., 2009). Therefore, catecholamine (such as ISO)-induced cardiac remodeling is appropriate to evaluate AuNPs-induced cardiotoxicity under pathological conditions *in vivo*.

In the present study, we evaluated the biological distribution of AuNPs after repeated intravenous administration, their effects on cardiac function and whether they would lead to cardiac hypertrophy, cardiac fibrosis and cardiac inflammation in normal mice. Furthermore, we investigated the biodistribution of AuNPs and their effects on cardiac function, cardiac hypertrophy, cardiac fibrosis and cardiac inflammation under pathological condition with an ISO-induced mouse model of cardiac remodeling.

2. Methods

2.1. Synthesis and characterization of the 13 nm AuNPs

The AuNPs were prepared by the citrate reduction method according to the reference with minor modifications (Frens, 1973). A 100 mL aqueous solution of $HAuCl_4$ (1 mM) was brought to the boil with vigorous stirring, and then 10 mL trisodium citrate solution (38.8 mM) was added quickly. After the solution color changed to deep red, the solution was refluxed for an additional 15 min. Ten mg of PEG-5000 was added to 10 mL of above aqueous solution, and stirred for 24 h to complete the ligand exchange (citrate to PEG). The morphology and size of the AuNPs were evaluated using transmission electron microscopy (TEM, JEM-200CX, Jeol Ltd., Japan). The surface charge of the nanoparticles (zeta potential, mV) and size distribution were determined using a ZetaSizer Nano series Nano-ZS (Malvern Instruments Ltd., Malvern, UK). The PEGylated AuNPs suspension was sonicated for 5 min before use.

2.2. Establishment of cardiac remodeling animal model

Our investigation was approved by the Biomedical Research Ethics Committee of Peking University (LA 2010-048) and strictly adhered to the American Physiological Society's "Guiding Principles in the Care and Use of Vertebrate Animals in Research and Training". 12-week-old male BALB/c mice were from the Animal Department of Peking University Health Science Center (Beijing, China). Mice were housed in groups of four and maintained on a 12 h dark/light cycle in a room with controlled temperature (25 ± 2 °C). Mice had free access to food and water.

Cardiac remodeling model was established by subcutaneous injection of ISO (5 mg/kg/day, dissolved in saline, Sigma–Aldrich, St. Louis, USA) for 7 consecutive days. Twenty-four mice were randomly divided into four groups (six mice each group) to receive for 7 consecutive days: (i) vehicle group: daily administration PBS injected into the tail vein as control; (ii) AuNP group: daily administration of 810 μg/kg AuNPs injected into the tail vein for 7 consecutive days; (iii) ISO group: daily subcutaneous administration of 5 mg/kg of ISO; or (iv) ISO + AuNP group: daily subcutaneous administration of 5 mg/kg of ISO and 810 μg/kg of AuNPs injected into the tail vein. AuNPs were dissolved in PBS. The volume of injection was adjusted to 5 μl/g of mice weight. Echocardiography analysis was performed 1 day before the first injection for the baseline and 1 day after the last injection as the final examination. And then mice were anaesthetized and euthanized. The hearts were excised and weighted immediately. Each excised heart was cut into two halves and detected with histological and immunohistochemistry analysis and ICP-MS, respectively.

2.3. Echocardiographic analysis

Mice were anaesthetized with 1% isoflurane (Baxter Healthcare Corporation, New Providence, USA). Echocardiographic images were obtained by the Visualsonics high-resolution Vevo 770 system (VisualSonics, Incorporated, Toronto, Canada). Two-dimensional parasternal long-axis views and short-axis views were obtained at the level of the papillary muscle. Diastolic left ventricular posterior wall thickness (LVPWd) and systolic left ventricular posterior wall thickness (LVPWs) were measured to calculate the ejection fraction (EF) and fractional shortening (FS). All measurements were averaged from three consecutive cardiac cycles.

2.4. Quantitative histological analyses

Following sacrifice, the hearts were harvested and perfused in retrograde with cold phosphate-buffered saline (PBS), fixed with 4% paraformaldehyde for 8 h, dehydrated in 20% sucrose for 24 h and then embedded in paraffin. Serial sections (5 μm thick) were stained with hematoxylin and eosin (H & E) for morphological analysis, and/or picrosirius red for the detection of fibrosis. For morphometrical analysis, photographs of left ventricular sections cut from the same location of each heart were observed under 400× magnification (Leica Microsystems Imaging Solutions Ltd., Cambridge, UK). Interstitial fibrosis was visualized with picrosirius red staining, and the cardiac fibrosis volume fraction was calculated as the ratio of the stained fibrotic area to total myocardial area.

2.5. Immunohistochemistry analysis

Paraffin heart sections were deparaffinized in xylene and re-hydrated. Antigen retrieval was achieved by boiling the slides in citrate solution for 10 min and slides were then washed with PBS. After quenching endogenous tissue peroxidase activity with 3% H_2O_2 for 10 min, the slides were then washed in PBS and samples blocked in PBS containing 5% goat serum albumin at 37 °C for 1 h. Primary antibodies to detect mouse CD45 (for hematopoietic stem cells and all cells of hematopoietic origin, except erythrocytes with rat anti-mouse CD45, 1:50 dilution, BD Pharmingen), mouse Mac-3 (for macrophages with rat anti-mouse Mac-3, 1:50 dilution, BD Pharmingen), were applied overnight at 4 °C in PBS. The samples were washed in PBS and then sequentially incubated with DAB Kit (ZSGB, Beijing, China) for 1 h in the next day. The peroxidase reaction was visualized using 3,3′-diaminobenzidine tetrahydrochloride (DAB) and slides were counterstained with hematoxylin. All images were analyzed using a color image analysis system (Image Pro Plus 6.0, Media Cybernetics Inc., Silver Spring, MD).

2.6. ICP-MS

The tissue concentrations of AuNPs were assessed by quantitative inductively coupled plasma mass spectrometry (ICP-MS). One day after the last injection, mice were anaesthetized, euthanized and hearts was excised and weighed. Hearts were then digested in aqua fortis (nitric acid:hydrochloric acid 3:1). After adjusting the solution volume to 2 ml using 2% nitric acid and 1% hydrochloride acid (1:1), Au content assays were performed using an ELAN DRC e ICP-MS instrument (Perkin Elmer, Massachusetts, USA).

2.7. Statistical analysis

Data are summarized as means ± SEM. Differences in data between groups were compared using Prism 5 (GraphPad Software Incorporae, La Jolla, CA, USA) with Student's unpaired two-tailed *t*-test. $P < 0.05$ was considered statistically significant.

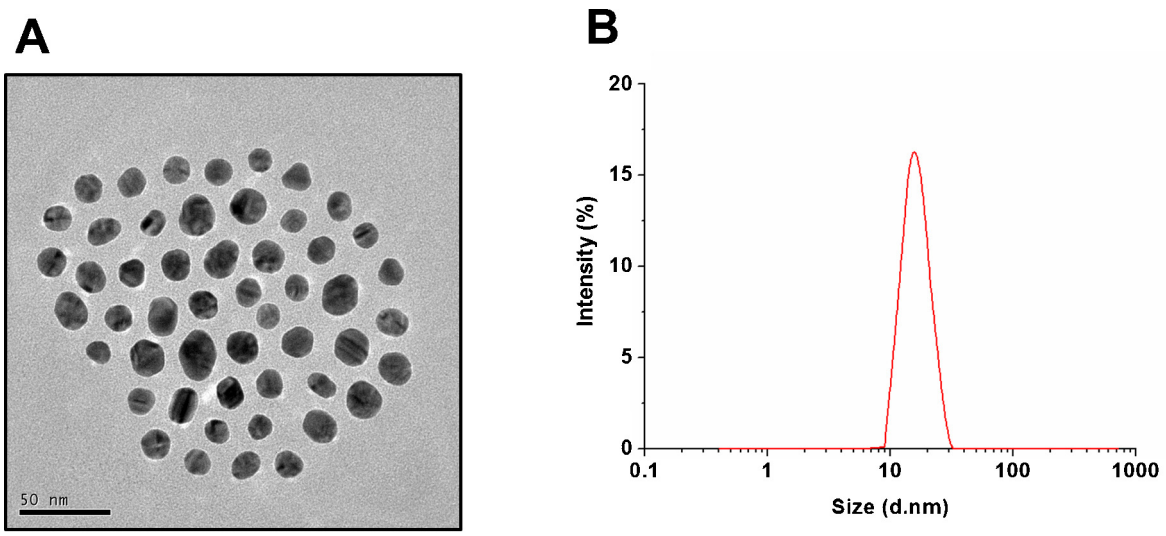

Fig. 1. Characterization of Au13-PEG. (A) Transmission electron microscopy (TEM) images of Au13-PEG. (B) Au13-PEG size distributions.

3. Results

3.1. Characterization of AuNPs and cardiac distribution of Au under physiological and pathological conditions

PEGylated AuNPs were monodispersed under TEM detection, with a mean diameter of ~13 nm (Fig. 1A and B). The hydrodynamic diameter of PEGylated AuNPs was about 15 nm, a slightly larger than the size measured by TEM, with zeta potential of −6.3 mV.

To mimic the potential biomedical applications of the AuNPs in terms of administration method, we intravenously injected the AuNPs suspension or PBS through the tail vein into healthy adult male BALB/c mice (Scheme in Fig. 2A). We determined the Au content in the hearts under physiological and ISO-induced pathological conditions. AuNPs have a moderate accumulation in the hearts in the control mice, with Au concentration of 334.9 ng/g tissue weight (Fig. 2B). Interestingly, AuNPs accumulation in the ISO-induced hypertrophic hearts increased six-fold compared with normal hearts (2220 ± 660 ng/g tissue vs. 330 ± 70 ng/g tissue, $P < 0.05$). These results indicated that AuNPs aggregated significantly in ISO-induced pathological hearts. The AuNPs accumulation in ISO-induced pathological hearts was further confirmed by TEM (Fig. 2C).

3.2. Effects of AuNPs on cardiac function under physiological and pathological conditions

As no research reported the effects of AuNPs on cardiac function, we studied whether AuNPs had any adverse effects on cardiac function. The left ventricular ejection fraction (EF) and fractional shortening (FS) were the major indicators to evaluate the cardiac contraction function, which were calculated from LVPWd and LVPWs measured by echocardiography. The EF and FS of AuNP group and AuNP + ISO group showed no difference of statistical significance from those of the vehicle group and ISO group, respectively, (Fig. 3A–D). These results indicated that AuNPs had no adverse effects on cardiac function under both physiological and pathological conditions.

3.3. Effects of gold nanoparticles on cardiac structure and remodeling under physiological and pathological conditions

After evaluating the potential effects of AuNPs on cardiac functionality, we then measured the effects of AuNPs on cardiac structure and remodeling process. The ratio of heart weight to tibia length (HW/Tibia) and diastolic left ventricular posterior wall thickness (LVPWd) were the leading indicators of cardiac hypertrophy. LVPWd (Fig. 4A and B) and HW/Tibia (Fig. 4C) had no difference of significance in the AuNP group versus vehicle group, suggesting that *in vivo* exposure to AuNPs didn't result in cardiac hypertrophy in normal mice. Furthermore, picrosirius red staining illustrated that AuNPs didn't induce cardiac fibrosis (Fig. 5A). The mice of ISO group and ISO + AuNP group exhibited significant increase in the HW/Tibia and LVPWd and cardiac fibrosis compared with vehicle group and AuNP group, respectively (Fig. 4D and E), indicating that ISO-induced cardiac remodeling model was successful. Based on this ISO-induced pathological model, the LVPWd (Fig. 4F) and HW/Tibia (Fig. 4G) were not statistically different between the ISO + AuNP group and ISO group. Likewise, quantitative analysis revealed cardiac fibrosis was not significantly different between ISO + AuNP group and ISO group (Fig. 5B). Taken together, treatment with AuNPs did not aggravate ISO-induced cardiac remodeling. These results suggested that AuNPs exposure did not alter cardiac structure under both physiological and pathological conditions.

3.4. Effects of AuNPs on cardiac inflammation under physiological and pathological conditions

The most important feature of inflammation is inflammatory cells infiltration. Immunohistochemical staining of CD45 positive ($CD45^+$) cells in the heart sections was performed to determine the numbers of total inflammatory cells. MAC-3 positive ($MAC\text{-}3^+$) cells were tested to determine the number of macrophages. First, H & E staining showed there was no overt sign of cardiocyte morphology alternations after exposure to AuNPs (Fig. 6A). No $CD45^+$ or $MAC\text{-}3^+$ cells were detected in the heart sections of AuNP group and vehicle group (Fig. 6B). Considering that AuNPs may lead to transient early inflammation (especially influx of leukocytes), total inflammatory cells, macrophages and leukocytes (Ly-6G positive cells) were tested in the heart sections taken from mice receiving AuNPs for 3 consecutive days. No $CD45^+$, Ly-$6G^+$ or $MAC\text{-}3^+$ cells were detected (Fig. S1). Taken together, these results indicate that AuNPs did not induce cardiac inflammation under physiological condition. Furthermore, we examined the effects of the AuNPs on ISO-induced pathological heart. ISO can significantly induce inflammatory cells infiltration in the heart (Murray et al., 2000). The $CD45^+$ or $MAC\text{-}3^+$ cells infiltrating in the hearts were obviously observed (Fig. 6C). However, the amount difference of $CD45^+$ cells or $MAC\text{-}3^+$ cells

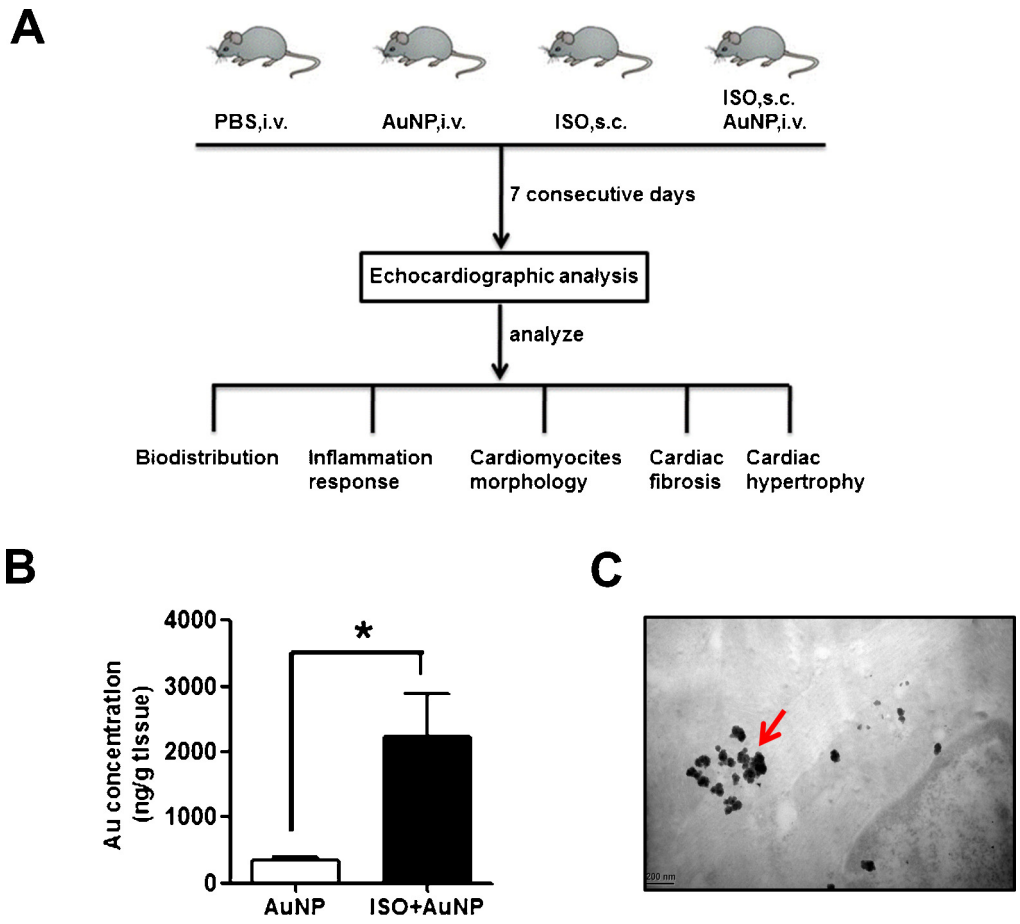

Fig. 2. Treatment of BALB/c mice with AuNPs and biodistribution of AuNPs in the heart. (A) Scheme of biodistribution and nanotoxicology experiment. 24 mice were randomized in four groups of six mice at the beginning of experiment. All mice in the vehicle group and AuNP group survived to the endpoint. Echocardiography analysis was performed 1 day before the first injection for the baseline and 1 day after the last injection as the final examination. And then mice were anaesthetized and euthanized. The hearts were excised and weighted immediately. Each excised heart was cut in half. One was used for inductively coupled plasma mass spectrometry (ICP-MS) analysis and the other was used for histological and immunohistochemical analysis. (B) Au contents in the heart under physiological condition and pathological condition. Au content was evaluated by ICP-MS. The values are expressed as ng/g tissue. $^{*}P < 0.05$, data represent means ± SEM. (C) TEM image of heart. Arrowhead shows AuNPs in the heart.

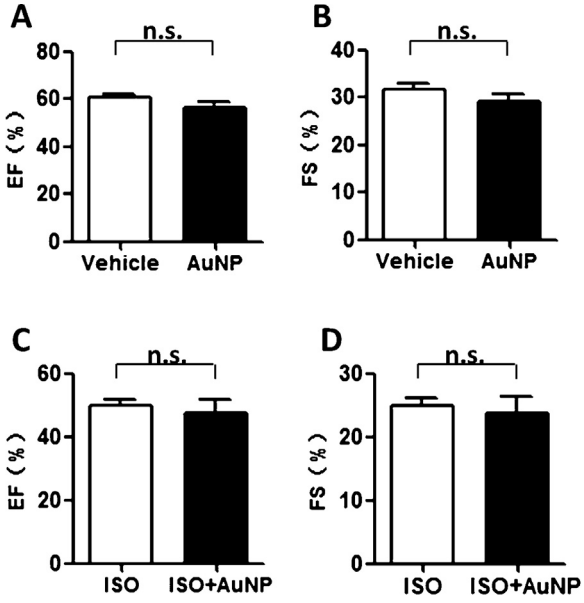

Fig. 3. The effects of AuNPs on cardiac function. Diastolic left ventricular posterior wall thickness (LVPW; d) and systolic left ventricular posterior wall thickness (LVPW; s) were measured. Ejection fraction (EF) and fractional shortening (FS) were calculated from these parameters. EF (A and C) and FS (B and D) were not significantly different in AuNP (−) and AuNP (+) mice received vehicle or ISO.

infiltrating in the hearts were not of statistical significance after exposure to AuNPs (Fig. 6D and E), suggesting that AuNPs did not exacerbate cardiac inflammation under pathological condition.

Supplementary data associated with this article can be found, in the online version, at http://dx.doi.org/10.1016/j.toxlet.2013.07.018.

3.5. Effects of AuNPs on myocardial apoptosis

Considering that 13 nm PEG-coated AuNPs were reported to induce apoptosis in the liver (Cho et al., 2009), we assessed whether AuNPs resulted in myocardial apoptosis. Our data showed that 13 nm PEG-coated AuNPs did not induce myocardial apoptosis (Fig. S2).

Supplementary data associated with this article can be found, in the online version, at http://dx.doi.org/10.1016/j.toxlet.2013.07.018.

4. Discussion

With the accelerating development and applications of AuNPs in disease diagnosis and drug delivery (Liu and Ye, 2013), the importance of assessing the potential risks of AuNPs to human health is growing. Polyethylene glycol (PEG) as modifying polymer can decrease immunogenicity and increase stability of drugs in the circulatory system (Veronese and Pasut, 2005). The coated PEG

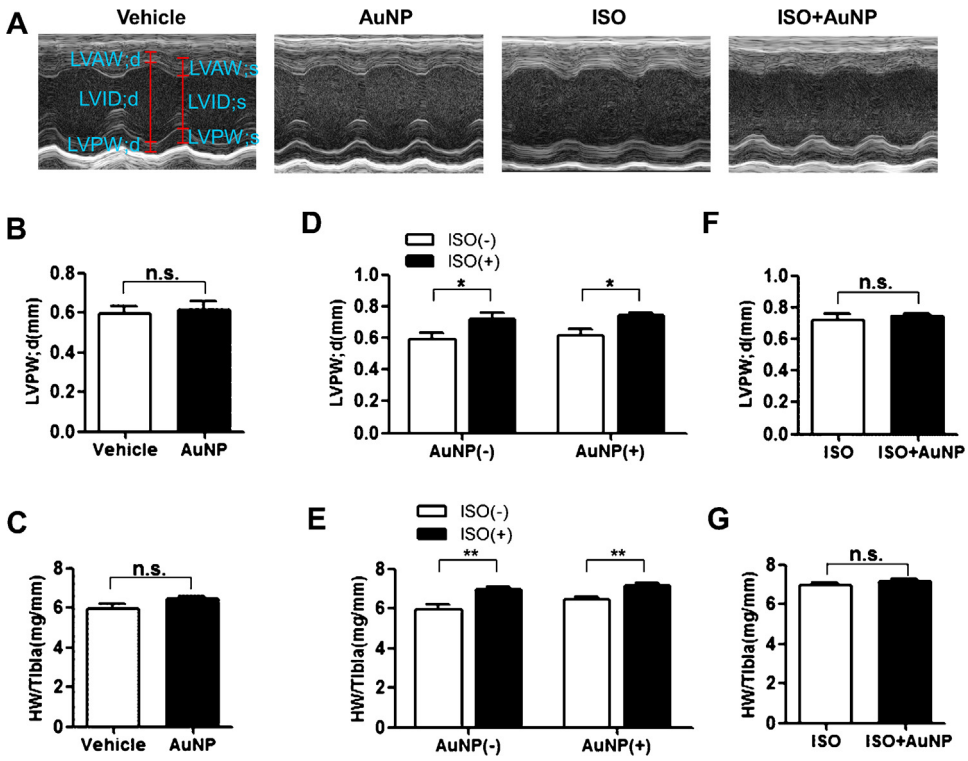

Fig. 4. The effects of AuNPs on cardiac hypertrophy. (A) Representative M-mode echocardiography images show left ventricular wall thickness and systolic function. (B) Diastolic left ventricular posterior wall thickness (LVPW;d) and (C) the ratio of heart weight to tibia length (HW/Tibia) were not significantly different in mice received vehicle or AuNPs. (D) Diastolic LVPW and (E) HW/Tibia of mice received vehicle, or ISO, or AuNPs, or ISO plus AuNPs showed that ISO induced cardiac hypertrophy. (F) Diastolic LVPW and (G) HW/Tibia were not significantly different in mice received ISO or ISO plus AuNPs. $^{*}P < 0.05$, $^{**}P < 0.01$. Data represent means ± SEM.

enhances the potentials of AuNPs in the medical applications. In the present study, we evaluated the effect of 13 nm PEG-coated AuNPs exposure on heart under both physiological and pathological conditions. First, the distribution of PEG-coated AuNPs in the heart was assessed in normal mice and ISO-induced model of cardiac remodeling mice. We found that AuNPs accumulation in the heart dramatically increased in ISO-induced pathological model mice compared with normal mice. Some ISO stimulation induced obviously myocardial inflammation in our study, consistent with some other studies (Davel et al., 2008; Sushama et al., 1990). Therefore, it is speculated that the AuNPs accumulation in the heart may be caused by the increased vascular permeability induced by ISO-mediated inflammation. Besides, macrophages play a central role in the uptake of AuNPs (Sadauskas et al., 2007), and may infiltrate in the heart with AuNPs after ISO treatment.

PEG-coated AuNPs administrated intravenously was shown to lead to acute inflammation and apoptosis in the liver after a single dose (Cho et al., 2009). Citrate-coated AuNPs damaged actin filaments, subsequently crippling the motility of cells and their proliferative and adhesive abilities *in vitro* (Pernodet et al., 2006). However, a great numbers of studies have shown that gold nanoparticles have no acute or subacute toxicity *in vitro* or *in vivo* (Connor et al., 2005; Lasagna-Reeves et al., 2010; Male et al., 2008). Although the heart is the major organ exposed to nanoparticles once the NPs enter the circulatory system, there are few data on the cardiac toxicity of NPs. Abdelhalim reported that the AuNPs of 10, 20 and 50 nm resulted in heart muscle disarray with a few scattered chronic inflammatory cells infiltrated and hemorrhage (Abdelhalim, 2011). However, in our study, the HE-stained sections of heart exhibited no changes in cardiocytes after AuNPs were

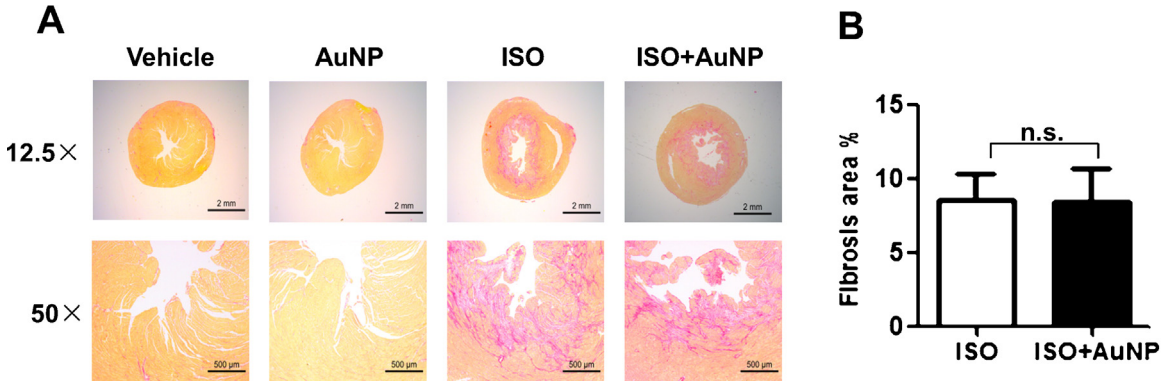

Fig. 5. The effects of AuNPs on cardiac fibrosis. (A) Representative micrographs of picrosirius red-stained sections of the ventricle. Red parts represent collagen. The scalebars of 12.5× images are 2 mm and those of 50× images are 500 μm. (B) Quantification of cardiac interstitial collagen content from picrosirius red-stained sections with results expressed as the ratio of collagen area to heart area.

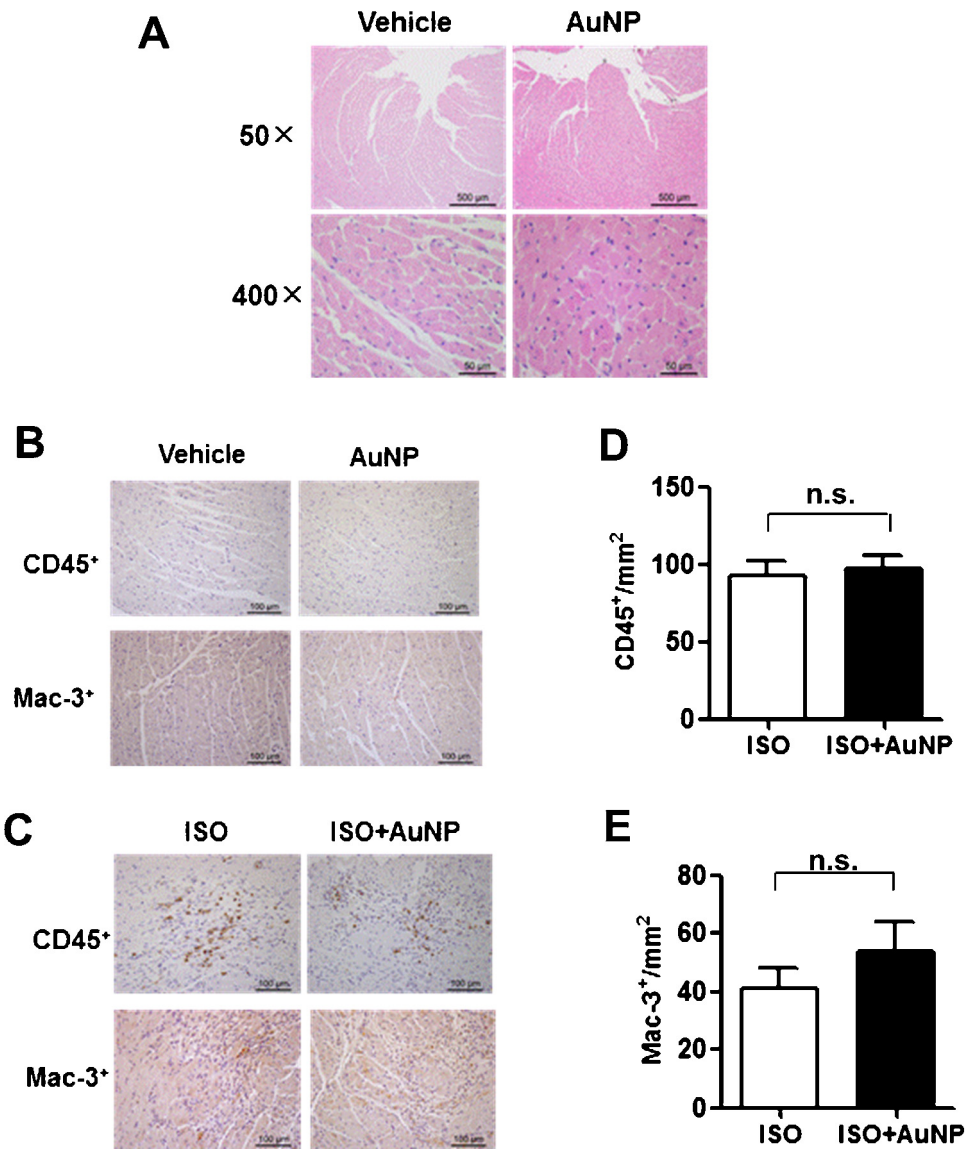

Fig. 6. The effects of AuNPs on ISO-induced cardiac inflammation. Injection of AuNPs alone did not result in the influx of inflammatory cells or extravasation of red blood cells in the heart. AuNPs had no effect on the number of inflammatory cells in the heart of mice received ISO. (A) Representative HE-stained sections of left heart. (B) Representative micrographs showing total inflammatory cells and macrophages in the heart of vehicle group and AuNP group; (C) Representative micrographs showing total inflammatory cells and macrophages in the heart of ISO group and ISO + AuNP group. (D) Quantification of $CD45^+$ cells. (E) Quantification of $MAC\text{-}3^+$ cells. The results are expressed as the ratio of the cell number to corresponding heart area.

injected intravenously for 7 consecutive days. Furthermore, the immunohistochemical examination of heart sections revealed that AuNPs did not induce inflammatory cells infiltration. These results are inconsistent with the observations of Abdelhalim (2011). Two possible reasons underlie the inconsistence. First, Wistar-Kyoto rats were employed in Abdelhalim's study, while BALB/c mice were employed in our study. Different species may response differently to the similar treatment. Second, naked AuNPs were used in Abdelhalim's study, while PEG-coated AuNPs were used in our study. PEG-coated AuNPs has been shown to cause less immune response than the naked AuNPs (Lee et al., 2013; Veronese and Pasut, 2005). Besides, the characteristic, the source of there AuNPs and the precise dose of AuNPs were not clearly described in Abdelhalim's study. These differences may cause different biological effect. Nevertheless, it is critical to further evaluate the complete biological effects of AuNPs under various biological conditions with careful characterization of the studied AuNPs.

Under physiological conditions, the left ventricular ejection fraction (EF) and fractional shortening (FS) of mice receiving AuNPs were not significantly different from those of vehicle, indicating that AuNPs did not affect cardiac function. HW/Tibia and LVPWd were not statistically different between mice receiving AuNPs and vehicle, revealing that AuNPs did not lead to cardiac hypertrophy. Furthermore, picrosirius red staining of heart sections illustrated that AuNPs did not induce cardiac fibrosis. Therefore, 13 nm PEG-coated AuNPs had no adverse effects on cardiac function and did not lead to cardiac remodeling in physiological condition. However, 22.5 nm PEG-coated AuNPs were reported to cause prolonged decrease in the mean arterial blood pressure in mice, while the endothelial function was not affected (Iversen et al., 2013). Apart from heart and vascular endothelium, the function of vascular smooth muscle can also affect the blood pressure. Thus, it is important to further investigate the effects of AuNPs on the vascular smooth muscle.

We employed an ISO-induced cardiac remodeling model, which is a well-developed pathological model of heart, to examine the effects of AuNPs on the cardiac remodeling process. After treated with ISO, mice exhibited significant increase in the HW/Tibia, LVPWd, clear cardiac fibrosis and cardiac inflammation. These results proved that the ISO-induced cardiac remodeling model in this study was successful. AuNPs accumulation in ISO-induced pathological hearts increased six-fold compared with normal hearts. However, the increased accumulation of AuNPs in the heart did not aggravate ISO-induced cardiac hypertrophy, cardiac fibrosis or cardiac inflammation. Taken together, 13 nm PEG-coated AuNPs had no adverse effects on the pathological heart.

In conclusion, we observed for the first time that 13 nm PEG-coated AuNPs have no obviously adverse effects on the heart under both physiological condition and ISO-induced cardiac remodeling model, indicating the profile of high safety of the PEG-coated AuNPs in the heart. Our results provide the basis for the further applications of AuNPs in the disease diagnosis, drug delivery and hyperthermia assisted disease therapy.

Conflict of interest statement

The authors declare that there is no conflict of interest.

Acknowledgements

This work was supported by grants from the National Natural Science Foundation of China (No. 30910103902, No. 81070078 and No. 81270157), the National Basic Research Program of China (Grant no. 2011CB503903) and Beijing Municipal Natural Science Foundation (7102158).

References

Abdelhalim, M.A., 2011. Gold nanoparticles administration induces disarray of heart muscle, hemorrhagic, chronic inflammatory cells infiltrated by small lymphocytes, cytoplasmic vacuolization and congested and dilated blood vessels. Lipids in Health and Disease 10, 233.

Cho, W.S., Cho, M., Jeong, J., Choi, M., Cho, H.Y., Han, B.S., Kim, S.H., Kim, H.O., Lim, Y.T., Chung, B.H., Jeong, J., 2009. Acute toxicity and pharmacokinetics of 13 nm-sized PEG-coated gold nanoparticles. Toxicology and Applied Pharmacology 236, 16–24.

Connor, E.E., Mwamuka, J., Gole, A., Murphy, C.J., Wyatt, M.D., 2005. Gold nanoparticles are taken up by human cells but do not cause acute cytotoxicity. Small 1, 325–327.

Davel, A.P., Fukuda, L.E., De Sa, L.L., Munhoz, C.D., Scavone, C., Sanz-Rosa, D., Cachofeiro, V., Lahera, V., Rossoni, L.V., 2008. Effects of isoproterenol treatment for 7 days on inflammatory mediators in the rat aorta. American Journal of Physiology Heart and Circulatory Physiology 295, H211–H219.

De Jong, W.H., Hagens, W.I., Krystek, P., Burger, M.C., Sips, A.J., Geertsma, R.E., 2008. Particle size-dependent organ distribution of gold nanoparticles after intravenous administration. Biomaterials 29, 1912–1919.

Dreaden, E.C., Austin, L.A., Mackey, M.A., El-Sayed, M.A., 2012. Size matters: gold nanoparticles in targeted cancer drug delivery. Therapeutic Delivery 3, 457–478.

Duncan, B., Kim, C., Rotello, V.M., 2010. Gold nanoparticle platforms as drug and biomacromolecule delivery systems. Journal of Controlled Release 148, 122–127.

Frens, G., 1973. Controlled nucleation for the regulation of the particle size in monodisperse gold suspensions. Nature Physical Science 241, 20–22.

Frey, N., Olson, E.N., 2003. Cardiac hypertrophy: the good, the bad, and the ugly. Annual Review of Physiology 65, 45–79.

Gunter, C., Dhand, R., 2002. Human biology by proxy. Nature 420, 509.

Huang, W.Y., Qian, W., Jain, P.K., El-Sayed, M.A., 2007. The effect of plasmon field on the coherent lattice phonon oscillation in electron-beam fabricated gold nanoparticle pairs. Nano Letters 7, 3227–3234.

Iversen, N.K., Nielsen, A.R., Wang, T., Baatrup, E., 2013. Intravascular infusion of PEGylated Au nanoparticles affects cardiovascular function in healthy mice. Human & Experimental Toxicology 32, 216–221.

Jeong, K., Kwon, H., Min, C., Pak, Y., 2009. Modulation of the caveolin-3 localization to caveolae and STAT3 to mitochondria by catecholamine-induced cardiac hypertrophy in H9c2 cardiomyoblasts. Experimental & Molecular Medicine 41, 226–235.

Khlebtsov, N., Dykman, L., 2011. Biodistribution and toxicity of engineered gold nanoparticles: a review of in vitro and in vivo studies. Chemical Society Reviews 40, 1647–1671.

Lasagna-Reeves, C., Gonzalez-Romero, D., Barria, M.A., Olmedo, I., Clos, A., Sadagopa, R.V., Urayama, A., Vergara, L., Kogan, M.J., Soto, C., 2010. Bioaccumulation and toxicity of gold nanoparticles after repeated administration in mice. Biochemical and Biophysical Research Communications 393, 649–655.

Lee, S., Kim, M.S., Lee, D., Kwon, T.K., Khang, D., Yun, H.S., Kim, S.H., 2013. The comparative immunotoxicity of mesoporous silica nanoparticles and colloidal silica nanoparticles in mice. International Journal of Nanomedicine 8, 147–158.

Liu, A., Ye, B., 2013. Application of gold nanoparticles in biomedical researches and diagnosis. Clinical Laboratory 59, 23–36.

Male, K.B., Lachance, B., Hrapovic, S., Sunahara, G., Luong, J.H., 2008. Assessment of cytotoxicity of quantum dots and gold nanoparticles using cell-based impedance spectroscopy. Analytical Chemistry 80, 5487–5493.

Murray, D.R., Prabhu, S.D., Chandrasekar, B., 2000. Chronic beta-adrenergic stimulation induces myocardial proinflammatory cytokine expression. Circulation 101, 2338–2341.

Oberdorster, G., Oberdorster, E., Oberdorster, J., 2005. Nanotoxicology: an emerging discipline evolving from studies of ultrafine particles. Environmental Health Perspectives 113, 823–839.

Patten, R.D., Hall-Porter, M.R., 2009. Small animal models of heart failure: development of novel therapies, past and present. Circulation: Heart Failure 2, 138–144.

Pernodet, N., Fang, X., Sun, Y., Bakhtina, A., Ramakrishnan, A., Sokolov, J., Ulman, A., Rafailovich, M., 2006. Adverse effects of citrate/gold nanoparticles on human dermal fibroblasts. Small 2, 766–773.

Prabhu, P., Patravale, V., 2012. The upcoming field of theranostic nanomedicine: an overview. Journal of Biomedical Nanotechnology 8, 859–882.

Rusyn, I., Gatti, D.M., Wiltshire, T., Kleeberger, S.R., Threadgill, D.W., 2010. Toxicogenetics: population-based testing of drug and chemical safety in mouse models. Pharmacogenomics 11, 1127–1136.

Sadauskas, E., Wallin, H., Stoltenberg, M., Vogel, U., Doering, P., Larsen, A., Danscher, G., 2007. Kupffer cells are central in the removal of nanoparticles from the organism. Particle and Fibre Toxicology 4, 10.

Sushama, K.S., Varghese, A., Muraleedharan, D., Menon, V.P., 1990. Protective action of aspirin in experimental myocardial infarction induced by isoproterenol in rats and its effect on lipid peroxidation. Indian Journal of Experimental Biology 28, 480–485.

van Berlo, J.H., Maillet, M., Molkentin, J.D., 2013. Signaling effectors underlying pathologic growth and remodeling of the heart. Journal of Clinical Investigation 123, 37–45.

Veronese, F.M., Pasut, G., 2005. PEGylation, successful approach to drug delivery. Drug Discovery Today 10, 1451–1458.

Yang, H., Sun, C., Fan, Z., Tian, X., Yan, L., Du, L., Liu, Y., Chen, C., Liang, X.J., Anderson, G.J., Keelan, J.A., Zhao, Y., Nie, G., 2012. Effects of gestational age and surface modification on materno-fetal transfer of nanoparticles in murine pregnancy. Science Reports 2, 847.